DOE/ER/60549--T1

DE91 002763

U.S. Department of Energy

FINAL REPORT

1.0 PROJECT TITLE: Lung Cancer Risk from Exposure to Alpha Particles and Inhalation of Other Pollutants in Rats

Project #: DE-FG02-87ER60549

Principal Investigator: Fredric J. Burns, Ph.D.

Organization: New York University Medical Center

Address: Department of Environmental Medicine
550 First Avenue
New York, NY 10016

Telephone: 914-351-5638

DISCLAIMER

FINAL REPORT

The goal of these experiments is to establish a quantitative correlation between early DNA damage and cancer incidence in a way that would be helpful for assessing the carcinogenic risk of radon alone or in combination with specific indoor pollutants. Rat tracheal epithelium has been exposed *in vivo* to ^{210}Po alpha particles in the presence and absence of NO_2 or cigarette smoke. The major accomplishments so far are: the design and implementation of a tracheal implant to simulate radon alpha particle exposure, the measurement of DNA breaks in a small 7.0 mm segment of the trachea exposed to external x-irradiation, the measurement of the rate of repair of the x-ray induced tracheal DNA strand breaks , the measurement of DNA strand breaks following inhalation of cigarette smoke or NO_2, the measurement of tracheal DNA strand breaks following exposure to high doses (>15 Gy) ^{210}Po alpha particle radiation, the assessment of the amount of mucous in the goblet cells and in the underlying mucous glands. So far we have been unable to detect DNA strand breaks in the tracheal epithelium as a result of exposure to NO_2 cigarette smoke or ^{210}Po alpha particles. We have developed a simple 'artificial' trachea consisting of rat tracheal epithelial cells growing on a basement membrane coated millipore filter. Experiments are proposed to utilize these artificial tracheas to eliminate the potential interference of increased mucous secretion and/or inflammation that can significantly affect the radiation dose from the alpha particles. Our model systems are in place and feasible. The lack of DNA strand breaks so far is puzzling but extremely interesting. The explanation of this interesting effect may provide insight into the mechanism of the epithelial response with relevance to the major goals of the project.

Initial findings indicated that the ^{210}Po α-particle radiation from the implants does not break the tracheal DNA as effectively as expected on the basis of radiation dose alone. Several possible explanations for the low DNA strand break efficiency of the implants are being considered including the following: 1) thicker than expected mucous barrier; 2) respiratory cell resistance to high LET induced DNA strand breakage; 3) faster than expected DNA repair; 4) excessive DNA-DNA crosslinking at high radiation doses; and 5) inaccurate dosimetry (unlikely but still possible because of the complex geometry). The data to be obtained as described below will enable us to distinguish between these possible explanations.

Design of the Implant

Several implant designs by 2 separate suppliers have been considered and tested. Design considerations included the shape of the implant, safety of handling the implant, stability of the implant in contact with body fluid, and stabilization of the implant in the center of the tracheal lumen. The implant is a 7.0 mm long hollow needle with an outside diameter of 1.0 mm fabricated of silver alloy. Dental wire protrudes through both ends and flares outward to stabilize the needle in the center of the airway (Figure 1).

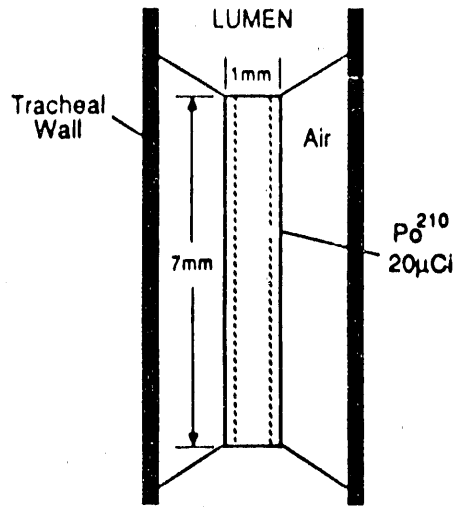

Figure 1. Diagram of the trachea showing an implanted needle in place. The diameter of the tracheal lumen is about 3.5 mm in the 10 week old rats used in the experiment. A tracheotomy is performed and the needle is placed in the lower portion of the trachea by trochar.

Calculation of Implant Source Strength

The implant is a needle or line source which serves as an irradiator. The needles are 7 mm in length and are uniformly coated with the alpha emitting isotope, polonium-210 applied by electroplating. The dose rate calculation at the surface of the tissue is based on the geometry of the needle being centered in the tracheal lumen with the radiation dose being delivered to the nearby tracheal wall. The range of the polonium-210 alpha particle in tissue is about 35 microns which is more than enough to reach the basal cell nuclei. The dose rate calculation is based on the expression that dose rate = particle flux x stopping power. This expression in the appropriate units can be written as follows:

$$dD/dt(rads/min) = 9.6 \times 10^{-7} F(\#/cm^2\ sec) \times dE/dR(Mev\ cm^2/g)$$

where dD/dt is the dose rate, F is particle flux at the tracheal wall, and dE/dR is stopping power. Given the stopping power of the alpha particles is about 340 mev cm^2/g, the above equation becomes:

$$dD/dt(rads/min) = 3.6 \times 10^4 F(particles/cm^2\ sec)$$

If the source is assumed to have a uniform distribution of activity per unit length represented by $S_L(\mu Ci/cm)$ then the differential flux at

point P at distance r from an incremental length of the source dy is given by:

$$dF = S_L dy/4\pi r^2$$

Integrating the foregoing expression over the length of the needle source gives for the flux, F, at point P the following expression:

$$F = S_L/4\pi \int dy/(y^2+h^2)$$

Evaluating at the midpoint of the source gives

$$F = (S_L/4\pi)(1/h)[(\tan^{-1}(L/2h) - \tan^{-1}(-L/2h)]$$

or

$$F = 2(S_L/4\pi)(1/h)\tan^{-1}(L/2h)$$

where L is the length of the needle and h is the distance from the needle. Since the isotope is plated on the surface of a metallic needle, the alpha particles emitted in the direction of the needle will be absorbed in the metal and will not contribute to the dose at the tracheal wall. Since one-half of the alphas are absorbed by the material of the needle, the flux at the tracheal wall will be reduced by a factor of one-half. If L=10 mm and h=1.0 mm then $\tan^{-1}(L/2h)=1.37$ and

$$F = 0.806 \times 10^5 \; S_L(uCi/cm)$$

Combining this expression for flux with the previous equation for dose rate gives for dose rate at h=1.0 mm:

$$dD/dt(Gy/min) = 0.263 \; S_L(uCi/cm)$$

Table 1. The relationship of tracheal wall dose rate to source strength as measured by amount of activity per unit length.

Source Strength (μCi/cm)	Dose Rate (Gy/min)
28.0	7.4
14.0	3.7
7.0	1.8
3.5	0.9

The above calculation refers to the tracheal dose at the midpoint of the source. The dose rate drops off with distance from the midpoint reaching about 50% of the midpoint dose at the ends of the needle. Sources were fabricated with the values of source strength indicated in Table 1 electroplated on the surface of the implantation needle. Liquid scintillation counting, track etch dosimetry and x-ray films were employed to verify the disintegration rates of the needles as they arrived from the manufacturer including; 1. calculation based on the known amount of activity plated on the needle and the geometry of the trachea, 2. calibrated film dosimetry to establish dose rate and distribution, and 3. track etch dosimetry as an independent measurement of absolute disintegrations and as a backup of the film dosimetry.

Dosimetric Evaluation of Radioactive Needles

The implants were placed on x-ray film for various times after which the films were evaluated by densitometry. A typical result is shown in Figure 2 which is a cross-section running perpendicular to the main axis of the needle.

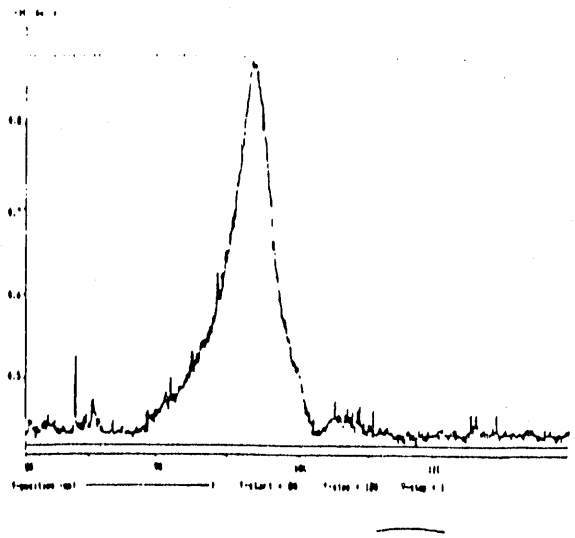

Figure 2. Densitometric cross section of film pattern produced by implant. The trace was made perpendicular to the long axis of the needle.

The pattern shown is what would be expected based on the inverse distance rule relating dose rate to distance from a needle source. The trace in Figure 3 runs parallel to the axis of the needle approximately at the peak of the pattern in Figure 2. This trace shows a uniform pattern of deposition of the radioisotope with some build up at the ends of the needle. If the distribution of radioactivity were exactly uniform, the pattern would be expected to peak at the midpoint and drop off near the ends reaching 50% exactly at each end. The pattern shown indicates that the activity is not uniformly distributed but actually has more activity near the ends of the needle that more than compensates for the expected decrease at the ends. The effect of the deposition non -uniformity is to produce a more uniform dose pattern along the length of the needle.

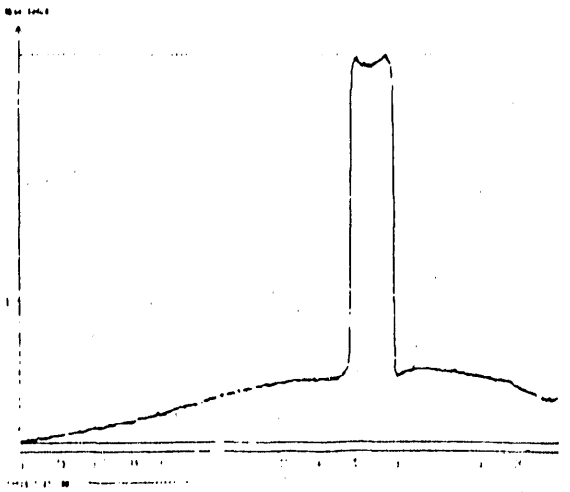

Figure 3. Densitometric trace along the long axis of the needle.

The film was calibrated in order to estimate absolute doses by exposing the same film to the calibrated neon ion beam at the Lawrence Radiation Laboratory's Bevalac in Berkeley, CA. Density units were converted into absolute dose in this way. We found that calibrating the film with electron radiation gave results that were wrong by nearly a factor of 50. The sensitivity of film is quite dependent on the linear energy transfer of the radiation. The film density showed excellent linearity with the amount of activity on the implants as seen in Figure 4.

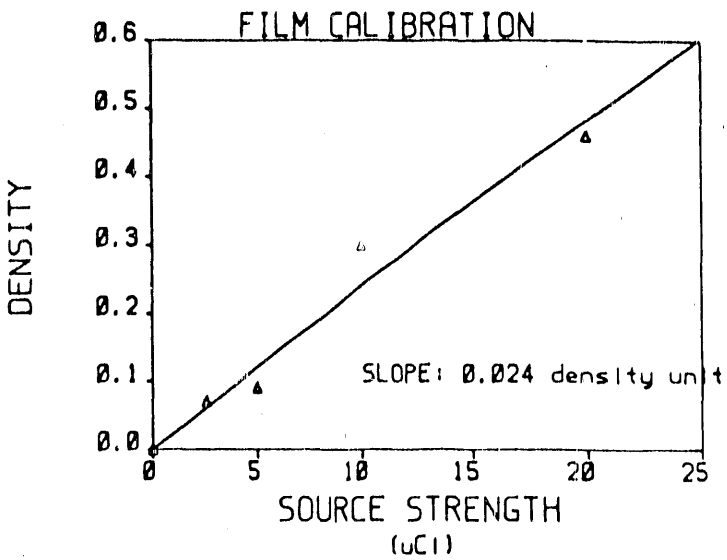

Figure 4. Calibration curve of the x-ray film exposed to needles with different amounts of radioactivity. The slope is 0.024 density units/μCi.

The track etch system is similar to the film system as a dosimeter. The difference with the track etch system is that each "bubble" may represent a single alpha particle, thereby obviating the need for comparative calibrations. Counting bubbles at different relative exposures gave the results shown in Figure 5. The data are reasonably linear, although the extrapolation to 0 intersects the y-axis at about 7 bubbles/unit field. This may be a limitation of the track etch method when counting small numbers of bubbles. The track etch patterns confirmed the excellent uniformity of the ^{210}Po on the needles (data not shown).

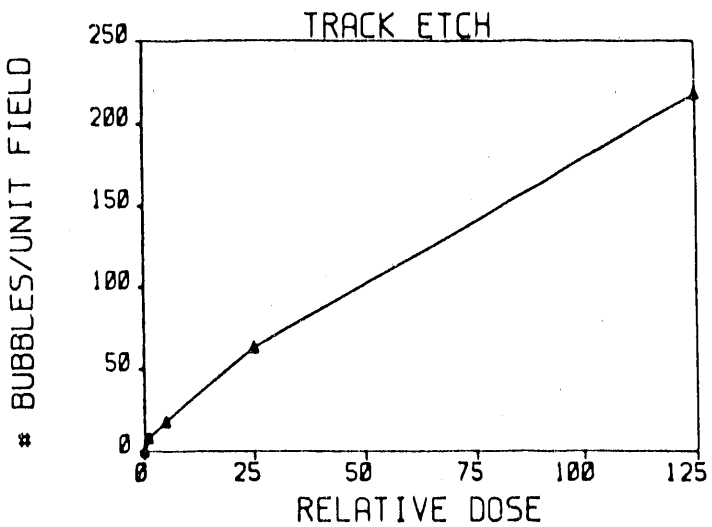

Figure 5. Calibration curve of the bubble pattern in polycarbonate exposed to the same needles. See text for conversion of the slope to dose rate per μCi at the surface of the source.

Unfortunately the ^{210}Po is not totally stable when plated on silver. The problem is the recoil energy of the ^{210}Po itself. The atom acquires sufficient energy to sometimes escape from the surface, sometimes taking other molecules with it. As a result we found that about 5% of the radioactivity was lost in a single 35 minute exposure in the animal. As this was considered unacceptable both as a potential long term hazard and as poor preservation of source strength, it was decided to coat the needles with 100 μg/cm^2 of gold. The effect of the gold layer on the energy spectrum of the alpha particles is shown in Figure 6.

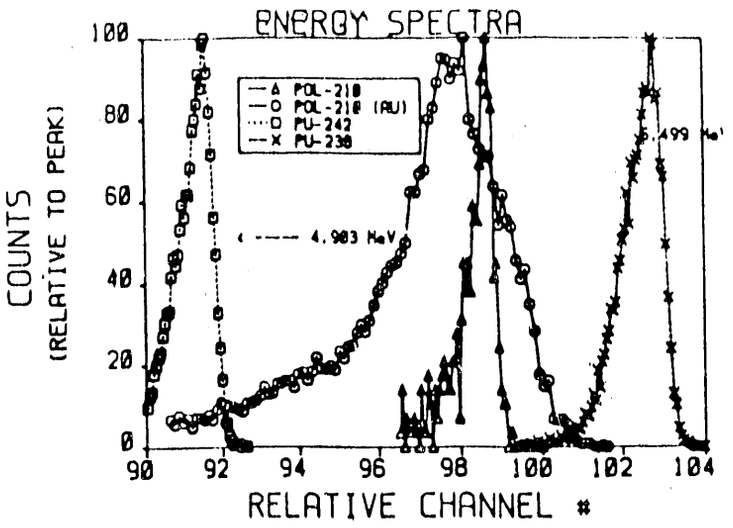

Figure 6. Alpha particle energy spectra showing effect of coating needles with 100 $\mu g/cm^2$ gold stabilizer. Standard spectra for known isotopes of plutonium are shown for comparison.

The major effect of the gold was to spread out the spectrum of energies; an insignificant shift (<1%) to lower energy also occurred. Reference spectra of plutonium-242 and plutonium-238 are shown.

External Irradiation of tracheal epithelium

External irradiation of the trachea has been employed as a means of verifying our methods. These data provide a comparison of external irradiation with results obtained by internal alpha particle irradiation. Rats were exposed externally to a high energy x-ray beam generated by bombarding a tantalum target with electrons from a Van de Graaff accelerator (1.8 MeV). The tracheal epithelium was prelabeled with ^{3}H-thymidine by means of 3 daily intraperitoneal injections of 1.0 $\mu Ci/g$ body weight. The x-ray beam was collimated appropriately and focussed on the trachea. Immediately after the exposures the tracheas were removed, and the epithelial cells were separated from the underlying stroma by trypsinization. The DNA was then subjected to alkaline elution with polycarbonate filters, and the elution profiles were analyzed by computer. The results indicated that the number of strand breaks induced by 3.0 Gy of surface dose would be detectible by current methodology. The methods utilized were originally worked out on skin, and these experiments have demonstrated that with minor modifications the same methods are applicable to the tracheal epithelium. These results have confirmed and established the feasibility of our methods for measurement of DNA strand breaks directly in the tracheal epithelium.

The DNA was subjected to alkaline elution once the cells were separated from the tracheal wall by 12 to 18 hr of trypsinization at 2°C. The actual separation was done with the help of a dissecting microscope to verify that only the epithelial cells were present. The epithelial cells were seen to separate in large sheets. These sheets were removed to separate vials and subjected to gently shaking and/or syringing in order to produce a more uniform cell suspension prior to elution. Some typical elution curves are shown in Figure 7 for tracheal cells irradiated with high energy x-rays. By allowing time to elapse between the end of the radiation exposures and start of the

trypsin incubation, the repair of tracheal DNA was studied.

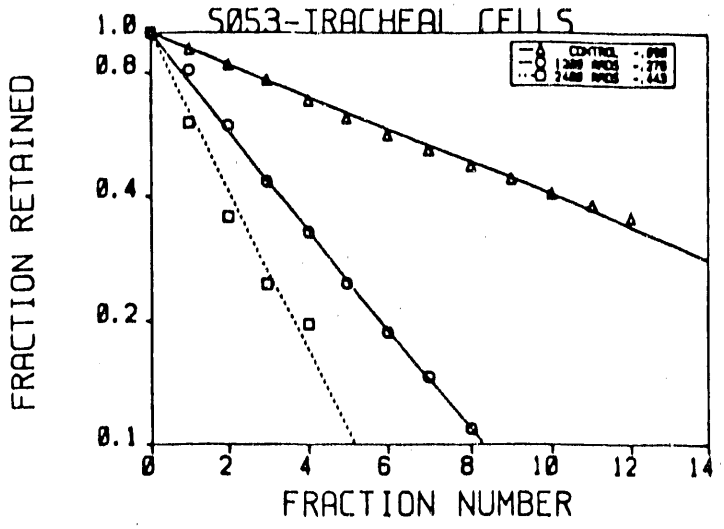

Figure 7. Alkaline elution profiles indicating relative elution rates of control and irradiated tracheal epithelial cells. The slopes of the lines are shown in the right part of the key box. The rats were irradiated externally with high energy x-rays.

Repair appears to follow a biphasic pattern with an initial phase exhibiting a halftime of about 15 min and a later, slower phase with a halftime of about 60 min. (Figure 8).

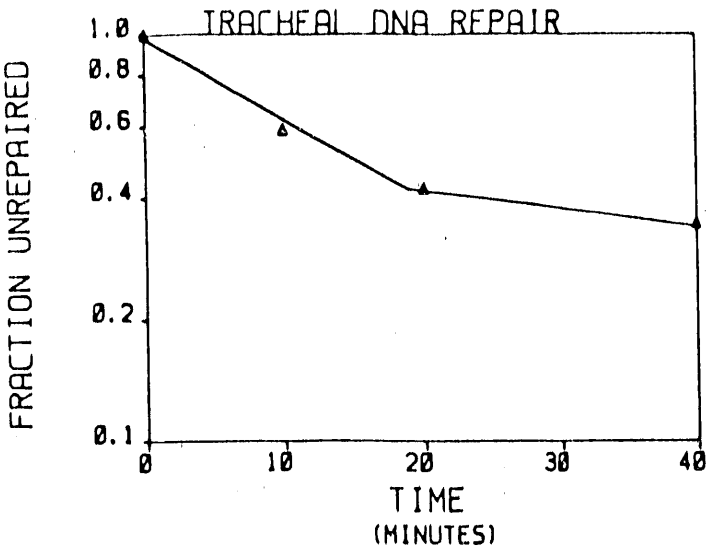

Figure 8. The repair of rat tracheal cell DNA as a function of time after irradiation with external x-rays.

Comparable data for rat epidermis exposed to electrons is shown in addition to the data for the rat tracheas in Figure 9. The slopes indicate that the trachea may be a little less sensitive to the radiation than the epidermis, but the difference could easily be explained by repair during the greater time required to dissect tracheas in comparison to skin (about 6 min versus about 3 min). The repair of DNA strand breaks in epidermis exhibits an initial halftime of about 15 min, but there was no evidence of a second slower phase.

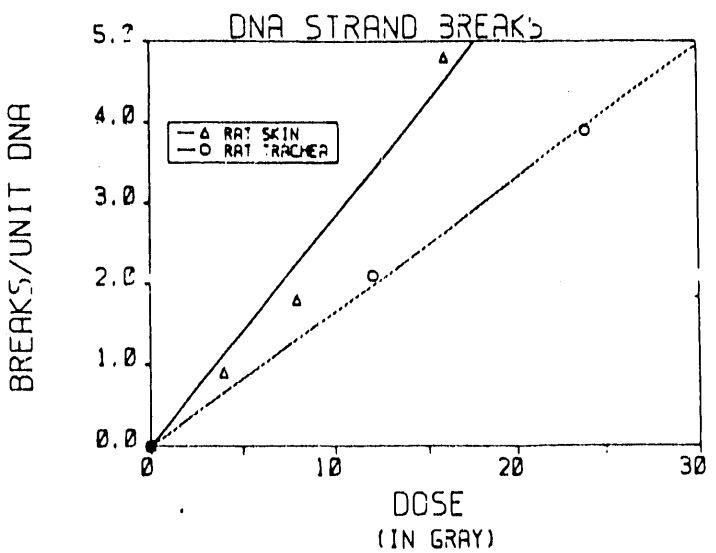

Figure 9. DNA strand breaks as a function of radiation dose in rat skin and tracheal epithelium as indicated. The skin was irradiated with electrons and the trachea was irradiated with x-rays.

DNA strand breaks in ^{210}Po exposed respiratory epithelium

Initial DNA strand break data in rat tracheal epithelium exposed to ^{210}Po needle implants is shown in Figure 10.

Contrary to expectation the slope in the treated tracheas was higher than control, although only by a small amount. Nevertheless we had expected the slope in the treated tissue to be much less than control based on the results for external radiation shown in Figure 8.

The results in Figure 10 are surprising and difficult to explain, so it was decided to employ a positive control in all experiments. The positive control was exposed to external high energy x-ray at a dose of 12 Gy.

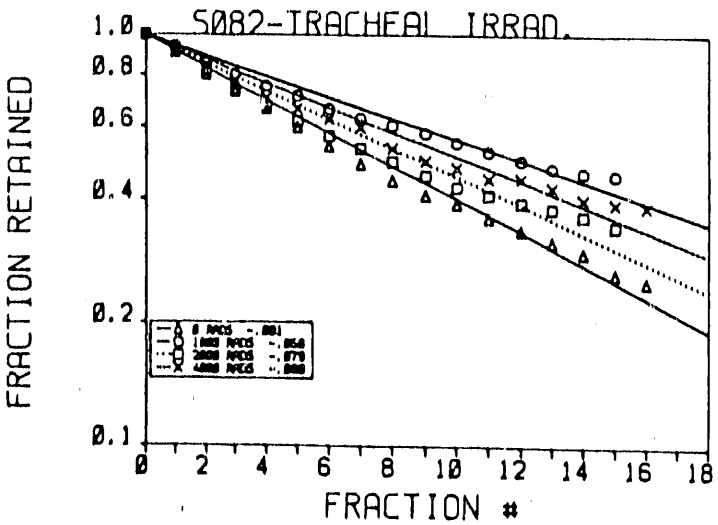

Figure 10. Elution profiles for rat tracheal DNA exposed by tracheal implantation to ^{210}Po alpha particles. The DNA was labeled with ^{3}HTdR. The dose was given in 35 minutes.

There is no evidence of strand breaks in the epithelium exposed by ^{210}Po implant even to a dose more than 3 fold greater than given to the positive controls. Another repeat indicated that perhaps the implant may have reduced the elution slope slightly, but the lack of a clear dependence on dose indicated that the decrease was probably not significant. Even so we were expecting the elution curve of the ^{210}Po irradiated cells to be shifted to the left and below the positive control curve; a result that clearly did not occur (Figure 11).

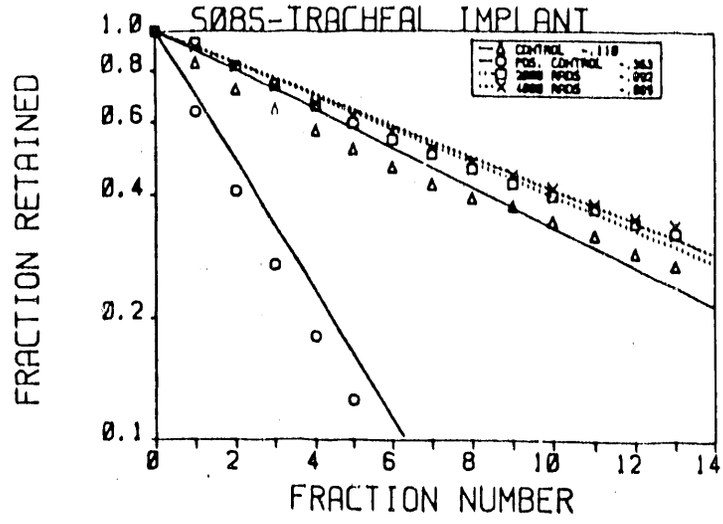

Figure 11. Elution profiles of rat tracheal DNA exposed to ^{210}Po alpha particles and to external x-rays (positive controls).

One possible explanation for these results is that the alpha particles were unable to reach the basal cell DNA because of an absorbing layer consisting of mucous and the tall columnar cells that comprise much of the respiratory epithelium. The original experiments utilized ^{3}HTdR which labels only the proliferating cells nears the basement membrane. These cells are presumably the stem cells and were of interest because they are more likely to be at risk for carcinogenesis than the relatively well differentiated cells located distal to the basement membrane.

By utilizing a fluorometric assay, we assayed all epithelial DNA, including non-dividing cells, not just the dividing basal cell DNA. These results are shown in Figure 12.

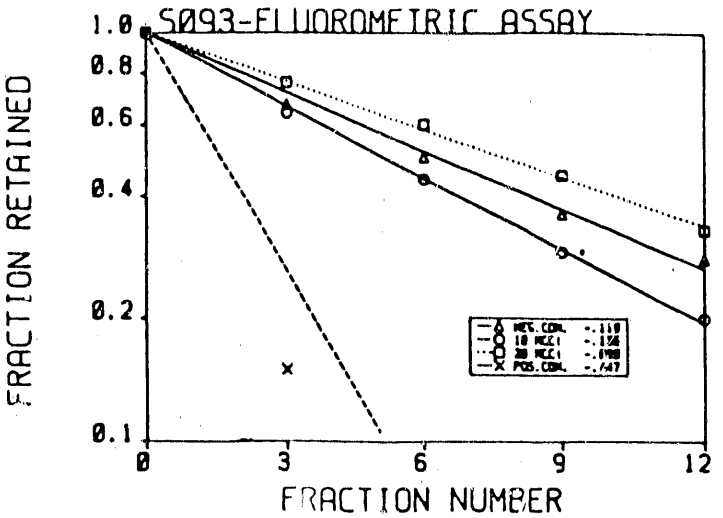

Figure 12. Elution profiles of rat tracheal DNA exposed to ^{210}Po alpha particles and to external x-rays. The DNA was quantified by use of a fluorescent dye.

These results are virtually the same as seen for the non-fluorometric assay; a clear slope increase for the positive control and no effect of the ^{210}Po implants. The implication of these results is that neither the DNA in the basal cells nor the DNA in the superficial cells is broken by the ^{210}Po alpha particles.

These are puzzling results and imply either that some absorbing material is intervening between the implant and the epithelial cells, eg. a mucous layer, or the epithelial DNA is responding in an unexpected way to relatively high doses of high LET radiation. We have performed some experiments intended to provide clues concerning the explanation of this interesting effect.

The mucous layer as a radiation absorber

Our first inclination was to hypothesize that the mucous barrier was somehow preventing the alpha particles from penetrating. There is normally a thin layer of mucous covering the tracheal epithelium. The thickness of this layer is difficult to estimate accurately but in normal circumstances it is not usually thicker than about 2-4 μ in the rat. The range of the ^{210}Po alpha particle is about 35 μ in unit density material. Routine radioautographs to determine the location of the cells taking up the $^{3}HTdR$ revealed tracks of some contaminating ^{210}Po particles to be more than adequate to penetrate not only the mucous layer but the entire epithelium. If mucous were the explanation for the lack of effect of the alpha particles on the DNA, it would have to be much thicker than normal, i.e. at least 20 μ in thickness. There is reason to believe that the tracheal mucous layer would not exceed 5 u even if all available mucous from goblet cells and mucous glands were to be utilized.

Several experiments were conducted to obtain more information on the amount and distribution of mucous in the tracheal lumen during exposure to the implants. In one

experiment we stained the tissue sections from the relevant region of the trachea with periodic acid Schiff (PAS), a procedure that shows mucous as dark blue. Prior to implantation we estimated that about 10% of the respiratory cells lining the lumen were goblet cells, i.e. cells containing a large globule of mucous. After the implant was removed, the proportion of cells exhibiting globules of mucous dropped to nearly 0%. Presumably the presence of the implant had caused the goblet cells to discharge their stored mucous. In addition the sub- epithelial mucous glands were devoid of stored mucous. Apparently all of the available mucous was discharged by the physical presence of the implant. The discharge occurred irrespective of whether the implant was radioactive. The question still to be resolved is: what is the total mass of mucous discharged and is it enough to provide a barrier to prevent the ^{210}Po alpha particles from reaching the DNA of the underlying epithelial cells?

Conventional histological procedures, such as, formalin fixation, and dehydration, remove most of the mucous so that the mucous outside of cells, eg. on the ciliated surface of the tracheal airway is difficult to study. We utilized frozen sections in an attempt to determine if large quantities of mucous can be found in the tracheal lumen. So far these studies have been negative. The thickest mucous layer documented so far was about 4 μ thick, although occasional large aggregates of mucous-like material have been found sometimes mixed with red blood cells localized near the ends of the implants where stabilizing wires make contact with the tracheal wall. These studies are continuing systematically to examine the mucous thickness as a function of time after implantation of a needle.

Another possibility is that the presence of the implant stimulates a vigorous inflammatory reaction and the accompanying edema may thicken the tissue sufficiently to block the alpha particles. To test this hypothesis we examined the tissue for evidence of edema and found none. Further we dosed the animals with dexamethasone, 4.0 mg/kg, as an inflammatory suppressant and then measured the amount of DNA strand breakage in the respiratory epithelium following exposure to about 10 Gy of alpha-radiation dose. The results, shown in Figure 13 indicate that suppression of inflammation had no effect on the amount of DNA strand breakage.

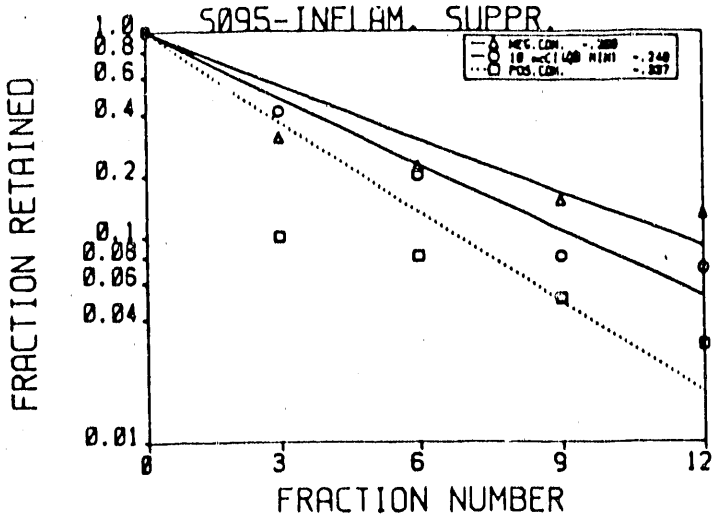

Figure 13. Elution profiles of rat tracheal DNA exposed to ^{210}Po alpha particles and to external x-rays. Rats with implant (labeled 10 mCi) were treated with 4.0 mg/kg dexamethasone to inhibit the inflammatory response.

Rat tracheal epithelial (RTE) cells in vitro

Experiments are in progress utilizing rat tracheal epithelial cells in vitro as a model system to determine if the respiratory DNA is somehow resistant to breakage by the action of high doses of alpha particles. These cells were obtained from Dr. Ann Marchok at Oak Ridge National Laboratory. These experiments have given negative results so far, but it is difficult to estimate the dose to cells growing on a flat surface from a radiation source that is cylindrical in shape. Accordingly we are fabricating what might be considered artificial tracheas of RTE cells growing on millipore filters treated with solubilized basement membrane. These filters will be rolled into the shape of a trachea and the source will be inserted inside. We have demonstrated the feasibility of growing RTE cells for short times (30 min) in this somewhat unconventional configuration.

DNA strand breaks in tracheas exposed to NO_2 or cigarette smoke

We have measured DNA strand breaks in the tracheas of rats exposed to either cigarette smoke or NO_2. These results are shown in Figure 14.

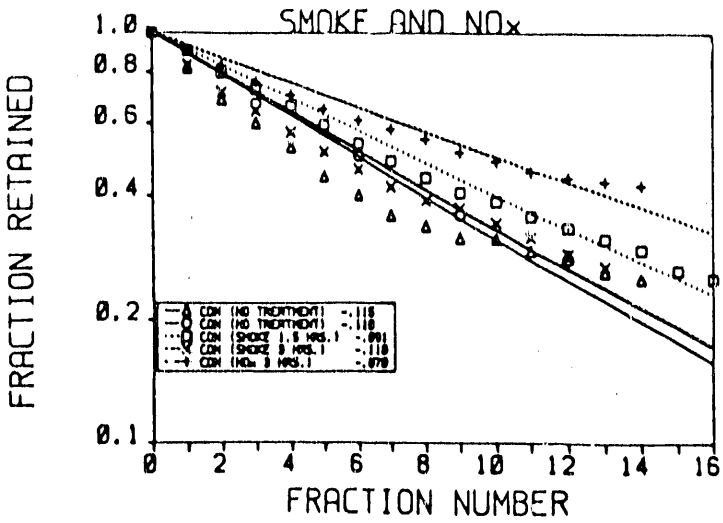

Figure 14. Elution profiles of rat tracheal DNA from animals exposed to cigarette smoke or NO_2. Exposure duration was either 1.5 or 3.0 hrs per day, 5 days per week for 2 weeks. The NO_2 concentration was 40 ppm.

So far none of the treatments have produced evidence of DNA strand breaks. The rats were exposed to 40 ppm of NO_2 for either 1.5 hr or 3 hr per day for 3 weeks and then examined 3 days later for the presence of DNA strand breaks with and without radioactive implants. None of the rats that received both cigarette smoke or NO_2 and ^{210}Po implants have exhibited evidence of DNA strand breaks. There is a tendency for the animals exposed to NO_2 to show less breakage than control as if the NO_2 may have produced cross-links that counteract strand breaks or have inhibited the expression of the strand breaks. We are continuing to study this interesting phenomenon.

Relevant rat skin studies

The induction and repair of DNA single strand breaks in rat epidermis was measured for electrons and neon ions with somewhat contrasting results. Alkaline elution profiles for different doses of electron radiation indicated essentially complete repair at all doses except 16 Gy. Plotting elution slopes (measure of DNA damage) as a function of electron dose gives a typical dose response and repair as indicated in Figure 15. By 2 hrs all DNA breaks were repaired at all doses. Comparable dose-response data for neon ions is shown in Figure 16. Rather than a monotonic increase in slope with dose, there is actually a decrease in response at 8 Gy. The effect at 4 Gy of neon ions was somewhat larger than seen for 4 Gy of electrons. At 2 hr there was little, if any, repair, but nearly complete repair occurred by 4 hrs. These results are new and indicate that DNA single strand break induction in rat epidermis after exposure to neon ions saturates at high doses ($\geq$ 8 Gy).

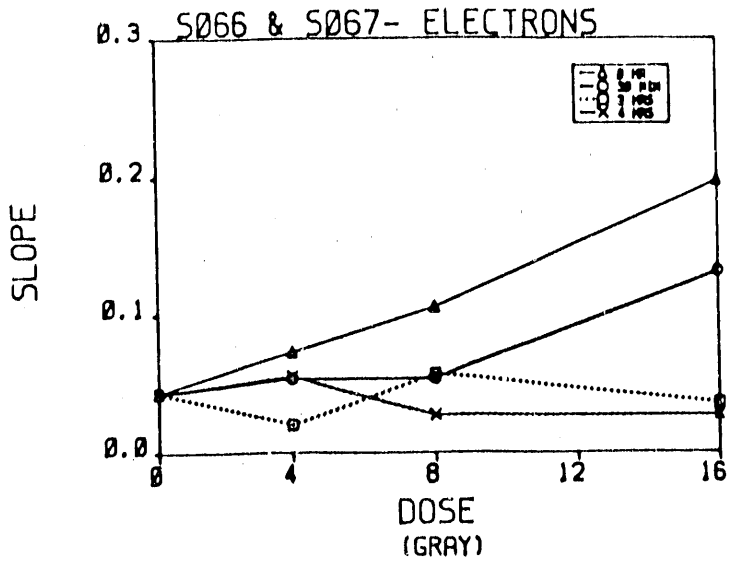

Figure 15. Elution slopes for rat skin DNA as a function of the dose of electrons (LET=0.34 kev/μ). The data were normalized to the average control slope at 0 Gy. Results for repair times of 30 min, 2 hrs and 4 hrs are also shown.

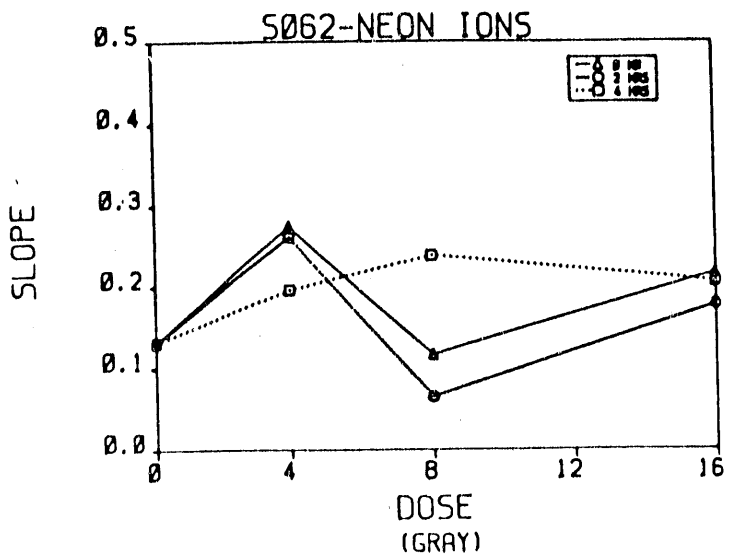

Figure 16. Elution slopes for rat skin DNA as a function of the dose of neon ions (LET=30 kev/μ). The data were normalized to the average control slope at 0 Gy. Results for repair times of 2 hrs and 4 hrs are also shown.

These results show that more DNA strand breaks per Gray at 4.0 Gy are produced by neon ions in comparison to electrons. Quantitatively the results are: neon ions, 0.29 breaks/unit DNA/Gy, and electrons; 0.19 breaks/unit DNA/ Gy, i.e. neon ions are about 1.53 times more effective than electrons per unit dose at 4 Gy. It should be noted

that the number of breaks in unirradiated controls was higher in the neon ion experiment than in the electron experiment possibly because of the extra handling involved in transporting the samples from California to New York. The incidence of DNA strand breaks above 4.0 Gy shows a consistent decrease indicating possible cross-linking or interference of expression at high doses. Also interesting and possibly significant is the relative lack of repair. At 2 hrs after irradiation virtually no repair has occurred, although a small amount of repair did occur by 4 hrs. These extremely interesting results raise the possibility that we have failed to see DNA strand breaks in the respiratory epithelium because the doses delivered were too high. We can not speculate at the present time why high doses of high LET radiation does not produce strand breaks to the same or greater extent as comparable doses of low LET radiation.

Generation of Inhalation Atmospheres

Cigarette smoke was generated using a 36 cigarette rotary wheel generator. Cigarettes were rotated into position and ignited by a thermistor. Main stream cigarette smoke is drawn into the exposure chamber via the venturi effect produced by chamber inlet air flowing perpendicular to the cigarette. The cigarette and generator are contained in a vented enclosure which ensures that only mainstream smoke enters the chamber.

Cigarette smoke sufficient to produce concentrations of 50 ppm and 25 ppm carbon monoxide (CO) were used in these experiments. For a 1.3 m^3 chamber operating with an air flow rate of 350 lpm this is equivalent to 2 packs (50 ppm CO) or 1 pack (25 ppm CO) of cigarettes every 90 minutes. Exposure was conducted for 3 hr/day, 5 days/wk.

NO_2 exposure was conducted using commercially available cylinders of nitrogen dioxide. A simple flow dilution technique was used to generate chamber atmosphere. Concentrations of 25 ppm and 10 ppm NO_2 will be used in these experiments. Although these concentrations are higher than those encountered in a typical home, 25 ppm was the concentration used in previous studies in this laboratory concerning the interaction of NO_2 with inhaled chemical carcinogens.

General Background

The harmful effects of inhaled radon on the human lung have been known since early in this century (1,2). Several models of radon dosimetry have led to the conclusion that most (on the order of 95%) of the radiation dose is attributable to decay of the short-lived daughters of radon rather than radon itself (3,4,5). It has also been shown that the radon daughters quickly attach to the aerosol particles and when inhaled the particle deposition pattern determines the distribution of radiation dose within the lung (6). Lack of information on the deposition is one reason why it is difficult to translate the known risks of lung cancer in uranium miners to risks in radon contaminated homes. Not only were the miners, generally speaking, heavy smokers but their environment was extremely dusty in comparison to most homes (7,8).

Experiments by Chameaud and colleagues have shown that tumors develop in the lung of rats exposed to radon in total or partial equilibrium with its daughters (9,10). In lifetime studies tumors were found in rats receiving as little as 65 WLM (working level months), i.e. about 32.5 rads, and the incidence increased almost linearly with dose. Tobacco smoke was found to be a significant cofactor in that the radiation dose to produce a given incidence of tumors was reduced and the tumors occurred earlier (11). Generally particulates, such as, ore dust or diesel exhaust, are irritants to the

pulmonary tissue and provoke inflammatory and proliferative responses in addition to the occurrence of epithelial hyperplasia and metaplasia in hamsters (12). The animal studies involving the inhalation of radon have shown clearly that the presence of dust alters pulmonary pathogenesis and that the radiation dose rate influences the probability of tumor development. The results cast doubt on the adequacy of the working level month idea as an index of carcinogenic risk, if exposure conditions differ radically as might occur in homes, for example.

Radiation Carcinogenesis

Our own studies of the dose-response relationship for cancer induction in different species by ionizing radiation (13,14) have shown the effect of spatial distribution of dose (15,16,17), the effect of time of exposure (18,19), and the importance of the linear energy transfer (LET) (20,21,22,23) and have led to important data for testing models of carcinogenesis. Rat skin was found to be capable of repairing the radiation-induced damage that leads to the formation of tumors for low LET radiation. For electron radiation the halftime of this repair was estimated on the basis of tumors counted to be about 3.5 hours (24,25). While many of the details of the radiation carcinogenic mechanism are uncertain, it is probable that two phases an involved (1) an initial interaction that alters the DNA in a way that is transmitted to daughter cells, and (2)subsequent changes in the altered cells or their progeny that cause them to acquire neoplastic properties (26,27).

We have developed a model of radiation carcinogenesis based largely on results obtained from irradiation of rat skin. In the model the tumor yield is related to molecular changes in the DNA occurring in phase 1, and alterations in phase 2 are assumed to exert approximately the same effect on tumor development independently of the radiation dose. The model is based on the fairly simple idea that a critical early event in the formation of a cancer cell is a chromosomal rearrangement derived from an interaction, probably an annealing, between broken DNA fragments (28,29). The result of the experiments have been surprisingly consistent with the expectations of the model and have given us encouragement to perform more critical tests (30,31,32).

DNA Strand Breaks in Carcinogenesis

In the model the number of DNA lesions (breaks) is assumed to be proportional to radiation dose, and the lesions are assumed to be independent if produced in different radiation tracks. When the LET of the radiation is low, e.g., electron radiation or x-rays, many tracks are necessary to produce a given dose, and the most likely interactions are those between lesions in different t acks. Hence, the chance of forming a rearrangement lesion (a chromosome rearrangement) will be the product of the lesion incidence with itself giving a dose squared term or BD^2. Repair becomes important for lesions in different tracks, for though they may be spatially close, there may be a separation in time so that a lesion may repair before a second one occurs.

On the other hand when the LET is high, as with radon and its daughters, hundreds of rads may be delivered by only one or two tracks per basal cell nucleus. Accordingly the lesions follow a geometrical alignment along particle tracks, and the most likely interactions are between lesions in the same track. The probability of an interaction is then linear in dose with a coefficient proportional to LET, i.e., CLD. It should be noted that not all chromosome rearrangements are carcinogenically relevant (many are undoubtedly lethal) and even the existence of a carcinogenically relevant chromosomal rearrangement does not mean that the cell is neoplastic.. Rather, the alteration is

envisaged to produce genetic instability that causes progressive acquisition of neoplastic properties as a result of additional alterations or recombinational rearrangements in subsequent mitoses. The dose response for tumor induction derived from the above considerations is:

$$Y=CLD+BD^2, \qquad (1)$$

where Y is the yield of cancers at a given time after irradiation (tumors per rat), D is the absorbed radiation dose, L is the LET and C and B are empirical constants.

Preliminary results for onset of epithelial cancers in skin, indicate a pattern that is consistent with the predictions of the linear quadratic equation based on evaluating constants with data from an earlier experiment with argon ions. Generally epithelial cancer yield as a function of time after exposure was fitted with a power function of the form

$$Y(t) = G\ t^n \qquad (2)$$

where t is elapsed time and n and G are constants. The argon and neon ion data have been fitted with n=2.2. For consistency these data have been fitted with the same power function (n=2.2) even though the data show a tending to plateau at longer times ($\geq$ 80 weeks). These are preliminary results and have not been confirmed histologically, although we expect the final results to vary little from the data shown.

Cancer yield per unit dose at 52 weeks for argon ions, electrons and neon ions are shown in Figure 17. Present data for electron radiation (symbol with error bars) have been supplemented with earlier data (no error bars). The data are expressed as yield per unit dose in order to estimate CL as the y-intercept and B as the slope in the equation:

$$Y(D)/D = CL + BD \qquad (1a)$$

The solid line shown was derived from a least square fitting procedure to the argon ion data. The dotted line for neon ions was derived solely from the argon ion result by assuming B and C remain the same and only L changes from 125 kev/μ to 30 kev/μ. This reduces the y-intercept from 0.055 tumors/rat/Gy for argon to 0.013 tumors/rat/Gy for neon. The actual neon ion data are positioned around this predicted line as strong confirmation that Equation 1a correctly accounts for the effect of LET on cancer induction in the rat skin system. The value of the slope, B, for argon and neon is 0.0060 tumors/rat/Gy^2.

Equation 1a, however, fails to predict correctly the response to electron radiation. The predicted line for electrons based on equation 1a (LET = 0.34 kev/μ) is shown just below the line for neon. The actual data for electrons (open squares) is much lower and to the right of the predicted line. The electron data are best fitted with a slope of B 0.0027 tumors/rat/Gy^2. The ratio of expected and observed slopes is 2.2 which implies the neon (and argon) are, 1.49 (1.49 = $\sqrt{2.2}$) fold more effective than electrons in producing 2 track alterations relevant to carcinogenesis.

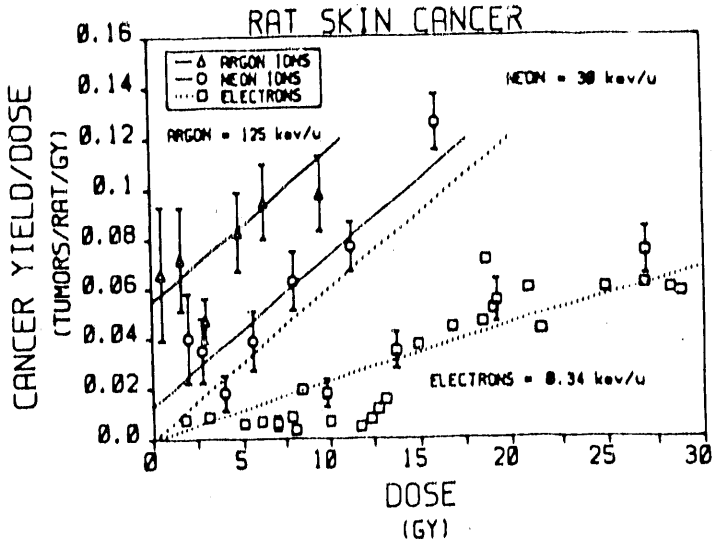

Figure 17. The incidence of rat skin cancer as a function of dose and linear energy transfer (LET). The results are expressed as cancer incidence per unit dose at 1 year to illustrate the effect of LET on the linear term. The LET of ^{210}Po alpha particles is approximately that shown for argon ions. For comparison results obtained with low LET electrons are also shown.

Another way to analyze these results, especially relevant to low dose extrapolation, is to consider the dose, D_e, where the linear and dose squared terms make equal contributions to the cancer yield. Based on the formula $D_e = (C/B)\ L$, these results are: D_e = 2.0 Gy and 8.3 Gy for neon and argon ions respectively. The neon ion dose-response ought to be predominately linear below 2 Gy and the argon ion data ought to be predominantly dose squared above 8.3 Gy. A similar response might be expected for ^{210}Po alpha particles since their linear energy transfer (LET) is quite high (> 100 kev/μ) being comparable or even higher than that of argon ions.

DNA Rearrangement and Oncogene Activation

The potential for moving oncogenes to genomic locations that would produce amplification or enchanced expression, provides a basis for understanding how radiation-induced DNA strand breaks could be involved in carcinogenic progression (33,34,35). The extent that carcinogens, other than radiation, break DNA as part of their carcinogenic action is not known.

Our preliminary data suggest the possibility that a known effect of radiation on target DNA - double strand breaks leading to chromosomal rearrangements and gene amplification - may be directly linked to myc gene activation found in these tumors. Activation of the myc oncogene has been shown to occur via gene amplification, rearrangement and enhance transcriptional activity in other systems (53,54). Our preliminary findings provide insight into the molecular lesion(s) associated with myc activation in radiation induced skin tumors (44).

The myc oncogene is especially interesting because it has been studied extensively in human tumors. The myc oncogene in Burkitt's lymphoma is consistently involved in a specific translocation of the second and third exons from chromosome 8 to chromosome 14 just downstream from an active immunoglobulin promoter region (55). Similar translocations leading to aberrant expression of myc have been seen in mouse plasmacytoma (56,57). The myc gene has been mapped to chromosome 7 in rat (58). The advantage of the rat skin radiation tumor system is the potential to study.

Despite rapid progress in the molecular biology of oncogenes and the mechanisms by which such genes may contribute to transformation, the connection between the wealth of biological and biochemical information regarding environmentally induced cancer and the molecular mechanisms leading to carcinogenesis is poorly understood. Research using the new tools of molecular biology applied to well established models of experimental carcinogenesis can provide the data needed to make this critical connection. The elucidation of the causal relationship between carcinogen effects and the mechanism of oncogene activation is of major importance in the theoretical understanding of carcinogenesis, as well as identification of putative carcinogens, determination of a mechanistic foundation for risk assessment analysis, and possible approaches to cancer prevention, early diagnosis, and intervention.

Recovery and Repair in Radiation Carcinogenesis of Rat Skin

An important question in radiation carcinogenesis is whether the carcinogenically relevant alterations are repairable as radiobiological lesions before being repaired or eliminated during aging. In an extensive series of studies, we have shown that such repair occurs and is quite effective if the LET of the radiation is low but does not occur for heavy ion irradiation where the LET exceeds 100 kev/micron. For multiple exposures of low LET radiation, the time between exposures is an important determinant of the carcinogenic effect of the radiation. We estimated on the basis of two doses that the repairable alteration was being removed with a halftime of about 2.5 hrs (59). In other experiments we showed that the effectiveness of this repair remained undiminished for as many as 52 exposures (60,61).

In another series of experiments radiation doses were given weekly for a year and tumors were plotted. There were two important findings of these studies; (1) repair continued to be effective for at least about 40 exposures (over 90 Gy was necessary to produce the same tumor yield that 12 Gy would produce in a single exposure) and (2) the exponent of the power function fitted to the temporal onset data jumped from about 2 for single exposures to more than 6. The increase in the time exponent tended to reverse the effects of fractionation repair, and may indicate that irradiation of early tumor cells accelerate progression to cancer.

Cell Proliferation in Carcinogenesis

Cell proliferation has long been suspected of playing a role in carcinogenesis, but its specific role remains to be established. Indirect evidence and logic suggest that cell division could play a role in carcinogenesis by converting initial alterations into a form that is genetically transmissible to daughter cells.

To test whether cell proliferation affects tumor yield, rat skin was exposed in the growing phase of the hair cycle when the epithelial cell population in the hair follicles and to some extent in the epidermis are in a rapid state of proliferation. The yield of tumors was not substantially different than for skin irradiated in the

resting phase of the hair cycle. We further examined this question by artificially stimulating cell proliferation in the hair follicles and surface epidermis, respectively, by hair plucking and cellophane tape stripping. The stimulation of proliferation was continued for 6 months without any affect on tumor yield. Perhaps the cells that were stimulated into proliferation were not the ones at risk for carcinogenesis.

Cell proliferation whether induced as a result of regenerative hyperplasia or by some other mechanism may play a critical role in converting initial molecular lesions to carcinogenically relevant genetic damage. Cell proliferation, prior to the repair of the carcinogen-induced critical lesion in DNA, is probably an essential step in the initiation of liver carcinogenesis as evidenced by the results from a single, non-necrogenic dose of several carcinogens, such as methylnitrosourea (MNU) (45), 1,2 dmethylhydrazine (DMH) (46) and diethylnitrosamine (DEN) (47). Similarly, cell transformation by radiation and viruses requires at least one round of cell proliferation prior to the repair of critical DNA damage (48). Cell proliferation may exert its crucial effect in chemical carcinogenesis not only by converting premutational alterations into mutations but also by contributing to the conversion of initiated cells to more advanced stages of carcinogenesis (49). Many chemical carcinogens like ionizing radiation are known to interact with DNA and to be cytotoxic at high doses, and the proliferative regeneration may accelerate carcinogenesis (50).

A further possibility for the role of cell proliferation in carcinogenesis has been postulated to explain the dose/response function of carcinogenesis during promotion in the initiation-promotion system of mouse skin and may be relevant to the present proposal (51). A variant of the multistage theory, this hypothesis suggests that any one or all of the stages prior to actual cancer could undergo clonal expansion. Such growth would effectively expand the population of cells at risk for conversion to the next stage. Clonal growth of intermediate stages could be the principal mechanism of action of tumor promoters and could be as important for determining the temporal onset of tumors as the carcinogen dose itself. In view of these possibilities, we propose to measure the rate of proliferation among the cells chronically exposed to the radiation in the nasal epithelium at early times after exposure.

Respiratory Carcinogenesis by Inhalation of Direct-Acting Alkylating Agents

In studies involving the respiratory tract at the NYU Department of Environmental Medicine a number of chemicals have been found to produce cancers by inhalation. Most of the neoplastic lesions occurred in the nasal mucosa, because reactive chemicals do not penetrate deeply into the lung. Most recently it was found that several of these direct acting carcinogenic chemicals, including dimethylcarbamylchloride and betapropriolactone directly stimulate cell proliferation in the nasal mucosa and the cancers exhibit a specific pattern of oncogene activation (44). The respiratory epithelium is not a static tissue. What little information is available for carcinogenic chemicals indicates the progressive occurrence of hyperplasia, squamous metaplasia, and dysplasia in varying degrees depending on the dose level. Such changes have been noted in animals dying with and without cancer following exposure to direct-acting alkylating and acylating agents, aldehydes (such as, formaldehyde), but little histopathological information is available for exposure to radon or radon daughters.

In an inhalation study with DMCC in rats, gradual histopathological changes in the respiratory epithelium were noted. Even before the appearance of tumors the respiratory epithelium exhibited nodular atypical basal overgrowth in which cells lost their polarity and acquired hyperchromatic nuclei. This was followed by invasive down growth

of tumor filling the nasal cavity. These changes appeared to be similar to the ones found during induction of squamous cell carcinoma of the bronchus. Formaldehyde-exposed animals, dying with tumor, showed severe dysplasia and squamous metaplasia at times with atypia and production of large amounts of keratin (52).

Lung Carcinogenesis by Pellet Implantation

The implantation of radioactive pellets has been shown to produce bronchogenic carcinoma in rats and mice with alpha, beta, and gamma radiation (37-43). Successful pellets were cylindrical in shape with the radioactive isotope electroplated to the exterior surface of the cylinder. For insertion into rat bronchi the pellets were hollow platinum cylinders, 5 mm in length, and 1.2 mm in diameter with a wall thickness of 0.2 mm. The material was platinum. The malignant tumor observed in these studies arose from the basal layer of the bronchial epithelium. The results showed significantly higher rates of squamous cell carcinoma induction for ionizing radiation than for chemical carcinogens inserted in the same pellets. The dose-response relationship found in these studies was very shallow in the sense that each increase in the dose by a factor of 10 only increased the tumor yield by about 10%. However, tumors occurred relatively early; the mean induction time being 344 days and the earliest induction time being 143 days.

REFERENCES

1. Bouchard, C., Curie, P. and Balthazard, V. Action physiologique de l'emanation du radium. C.R. Acad. Sci. 138: 1384 (1904).

2. Morken, D.A. Acute toxicity of radon. AMA Arch. Ind. Health 12: 435 (1955).

3. Altshuler, B., Nelson, N. and Kuschner, M. Estimation of lung tissue dose from the inhalation of radon and daughters. Health Phys. 10: 1137 (1964).

4. Cohn, S.H., Skow, R.K. and Gong, J.K. Radon inhalation studies in rats. Arch. Ind. Hyg. Occup. Med. 7: 508 (1953).

5. Shapiro, J. Radiation dosage from breathing radon and its daughter products. AMA Arch. Ind. Health 14: 169 (1953).

6. Shapiro, J. and Bale, W.F. A partial evaluation of the hazard of radon and degradation products. In: Quarterly Technical Report, University of Rochester Atomic Energy Project Report UR-242, p. 6, University of Rochester Press, Rochester, NY (1953).

7. Desrosiers, A.E., Kennedy, A. and Little, J.B. Rn-222 daughter dosimetry in the Syrian golden hamster lung. Health Phys. 35: 607 (1978).

8. Haque, A.K.M.M. and Collinson, A.J.L. Radiation dose to the respiratory system due to radon and its daughter products. Health Phys. 13: 431 (1967).

9. Chameaud, J., Perraud, R., Maasse, R., Nenot, J.C. and LaFuma, J. Lung cancer induced in rats by radon and its daughter nuclides at different concentrations. In: Biological and Environmental Effect of Low Level Radiation, Vol. II, IAEA Publication STI/PUB/409 Vienna (1976).

10. Chameaud, J., Perraud, R., Chetien, J., Masse, R. and LaFuma, J. Experimental study of the combined effect of cigarette smoke and an active burden of radon-222. In: Late Biological Effects of Ionizing Radiation, Vol. II, IAEA Publication STI/PUB/489 Vienna, (1978).

11 Chameaud, J., Perraud, R., Masse, R. and LaFuma, J. Contribution of animal experimentation to the interpretation of human epidemiological data. In: Proc. of International Conference on Radiation Hazards in Mining-Control, Measurement and Medical Aspects, Society of Mining Engineers, New York (1981).

12. Cross, F.T., Palmer, R.F., Filipy, R.E., Busch, R.H. and Stuart, B.O. Study of the combined effects of smoking and inhalation of uranium ore dust, radon daughters and diesel oil exhaust fumes in hamsters and dogs. Battelle Pacific Northwest Laboratory Final Report, PNL-2744/UC-48, National Technical Information Service, Springfield, VA (1978).

13. Albert, R.E., Newman, W. and Altshuler, B. The dose response relationships of beta-ray induced skin tumors in the rat. Radiat. Res. 15: 410 (1961).

14. Albert, R.E., Burns, F.J. and Bennett, P. Radiation-induced hair follicle damage and tumor formation in mouse and rat skin. J. Natl. Cancer Inst. 49: 1131-1137 (1972).

15. Albert, R.E., Burns, F.J. and Heimbach, R.D. Skin damage and tumor formation from grid and sieve patterns of electron and beta radiation in the rat. Radiat. Res. 30: 525-540 (1967).

Albert, R.E., Burns, F.J. and Heimbach, R.D. The effect of penetration depth on electron radiation on skin tumor formation in the rat. Radiat. Res. 30: 515-524 (1967).

17. Albert, R.E. and Burns, F.J. Tumor and injury responses of rat skin after sieve pattern x-irradiation. Radiat. Res. 67: 142-148 (1976).

18. Burns, F.J., Albert, R.E., Sinclair, I.P. and Bennett, P. The effect of fractionation on tumor induction and hair follicle damage in the rat skin. Radiat. Res. 53: 235-240 (1973).

19. Burns, F.J., Albert, R.E., Sinclair, I.P., Vanderlaan, M. The effect of a 24-hour fractionation interval on the induction of rat skin tumors by electron radiation. Radiat. Res. 62: 478-487 (1975).

20. Burns, F.J., Albert, R.E. and Heimbach, R.D. The RBE for skin tumors and hair follicle damage in the rat following irradiation with alpha particles and electrons. Radiat. Res. 36: 225-241 (1968).

21. Burns, F.J., Albert, R.E., Vanderlaan, M. and Strickland, P. The dose-response curve for tumor induction with single and split doses of 10 mev protons. Radiat. Res. 62: 598 (1975).

22. Burns, F.J., Albert, R.E., Bennett, P. and Sinclair, I.P. Tumor incidence in rat skin following proton irradiation in a sieve pattern. Radiat. Res. 50: 181-190 (1972).

23. Albert, R.E., Burns, F.J. and Heimbach, R.D. The association between chronic radiation damage of the hair follicles and tumor formation in the rat. Radiat. Res. 30: 590-599 (1967).

24. Vanderlaan, M., Burns, F.J. and Albert, R.E. A model describing the effects of dose and dose rate on tumor induction by radiation in rat skin. In: Biological and environmental effect of low-level radiation, Vol. I, Vienna: International Atomic Energy Agency, pp. 253-263, 1976.

25. Burns, F.J. and Vanderlaan, M. Split dose recovery for radiation induced tumors in rat skin. Intl. J. Radiat. Biol. 32: 135-144 (1977).

26. National Academy of Sciences. The effects on populations of exposure to low levels of ionizing radiation. Advisory committee on the biological effects of ionizing radiation (BEIR), National Research Council, National Academy of Sciences, Washington, DC, 1980.

27. Upton, A.C. Role of DNA damage in radiation and chemical carcinogenesis. In: Environmental Mutagens and Carcinogens, Proc. Third International Conference on Environmental Mutagens (Eds., T. Sugimura, S. Kondo and H. Takebe), U. Tokyo Press, Tokyo/Alan R. Liss, Inc., New York, 1982, pp. 71-80.

28. Leenhouts, H.P. and Chadwick, K.H. Radiation induced DNA double strand breaks and chromosome aberration. Theor. Appl. Genet. 44: 167-172 (1974).

29. Upton, A.C. In: Cancer: Achievements, Challenges and Prospects for the 1980's, Vol. 1 (Eds., J.H. Burchenal and H.F. Oettgen), Grune and Stratton, New York, pp. 185-198, 1981.

30. Chadwick, K.H. and Leenhouts, H.P. The rejoining of DNA double strand breaks and a model for the formation of chromosomal rearrangements. Int. J. Radiat. Biol. 33: 517-529 (1978).

31. Kellerer, A. and Rossi, H. A generalized formulation of dual radiation action. Radiat. Res. 75: 471-488 (1978).

32. Goodhead, D.T., Munson, R.J., Thacker, J. and Cox, R. Mutation and inactivation of cultured mammalian cells exposed to beams of accelerated heavy ions. IV. Biophysical interpretation. Int. J. Rad. Biol. 37: 135-167 (1980).

33. Preston, R.J. DNA repair and chromosome aberrations: The effect of cytosine arabinoside on the frequency of chromosome aberrations induced by radiation and chemicals. Teratogenesis Carcinogenesis and Mutagenesis 1: 147-159 (1980).

34. Kohn, K.W., Ewig, R.A.G., Erickson, L.L. and Zwelling, L.A. Measurements of strand breaks and cross links in DNA by alkaline elution. In: Handbook of DNA Repair Techniques, (Eds., Friedberg, E. and Hanawalt, P.), 1979.

35. Sawey, M.J., Hood, A.T., Burns, F.J., and Garte, S.J. Activation of K-ras c-myc oncogenes in radiation induced rat skin tumors. Submitted for publication.

36. Bradley, M.O. and Kohn, K.W. X-ray induced DNA double strand break production and repair in mammalian cells as measured by neutral filter elution. Nucleic Acids Research 7: 793 (1973).

37. Kuschner, M., Laskin, S., Christofano, E. and Nelson, N. Experimental carcinoma of the lung. In: Proceedings of the Third National Cancer Conference, p. 485, J.B. Lippincott Co., PA, 1957.

38. Lisco, H. Autoradiographic and histopathologic studies in radiation carcinogenesis of the lung. Lab. Invest. 8: 162 (1959).

39. Scott, J.K. and Thomas, R. Polonium: Induction of pulmonary tumors following intratracheal injection. University of Rochester Atomic Energy Project Quarterly Review, p. 30, 1957.

40. Cember, H. and Watson, J.A. Bronchogenic carcinoma from radioactive barium sulfate. A.M.A. Arch. Ind. Health 17: 230 (1958).

41. Temple, L.A., Willard, D.H., Marks, S. and Nair, W.J. Induction of malignant tumors by radioactive particles. Nature 183: 408 (1958).

42. Altshuler, B. Dosimetry from a 106-Ru-coated platinum pellet. Radiat. Res. 9: 626 (1958).

43. Laskin, S., Kuschner, M., Nelson, N., Altshuler, B., Harley, J. and Daniels, M. Carcinoma of the lung in rats exposed to the beta radiation of intrabronchial ruthenium-106 pellets: 1. Dose-response relationship. J. Natl. Cancer Inst. 31: 219 (1963).

44. Garte, S.J., Hood, A.T., Hochwalt, A.E., D'Eustachio, P., Snyder, C.A., Segal, A. and Albert, R.E. Carcinogen specificity in activation of transforming genes by direct-acting alkylating agents. Carcinogenesis, (in press).

45. Cayama, E. et al. Nature 275: 60 (1973).

46. Ying, T.S., et al. Chem. Biol. Interact. 28: 363 (1979).

47. Borek, C. and Sachs, L. Proc. Natl. Acad. Sci., USA 57: 1522 (1967).

48. Todaro, G.J. and Green, H. Proc. Natl. Acad. Sci., USA 55: 302 (1966).

49. Rajalakshim, S., et al. Chemical carcinogenesis: Interactions of carcinogens with nucleic acids. In: Cancer: A Comprehensive Treatise. I., 2nd Edition (Ed., Becker, F.F.), Plenum Press, 1982.

50. Burns, F.J. and Tannock, I.P. Cell and Tissue Kinetics 3: 321-334 (1970).

51. Burns, F.J., Vanderlaan, M., Snyder, E. and Albert, R.E. In: Carcinogenesis, Vol. 2, Mechanisms of Tumor Promotion and Co-carcinogenesis (Eds., Slaga, T.J., Boutwell, R.K. and Sivak, A.), Raven Press, New York, pp. 91-96, 1978.

52. Kuschner, M., Laskin, S., Drew, R., Cappiello, V. and Nelson, N. Arch. Environ. Health 30: 73 (1975).

53. Hayward, W.S., Neel, B.G. and Astrin, S.M. Activation of a cellular oncogene by promoter insertion in ALV-induced lymphoid leukosis. Nature 290: 475-480 (1981).

54. Yander, G., Halsey, H., Kenna, M. and Augenlicht, L.H. Amplification and elevated expression of c-myc in a chemically induced mouse colon tumor. Cancer Res. 45: 4433-4438 (1985).

55. Dalla-Favera, R., Bregni, M., Erikson, J., Patterson, D., Gallo, R.C. and Croce, C.M. Human c-myc oncogene is located on the region of chromosome 8 that is translocated in Burkitts lymphoma cells. PNAS 79: 7824-7827 (1982).

56. Stanton, L.W., Watt, R and Marcu, K.B. Translocation, breakage and truncated transcripts of c-myc oncogene in murine plasmacytomas. Nature 303: 401-406 (1983).

57. Harris, L.J., D'Eustachio, P., Ruddle, F.H. and Marcu, K.B. DNA sequence associated with chromosome translocations in mouse plasmacytomas. Proc. Natl. Acad. Sci. 79: 6622-6626 (1982).

58. Sumegi, C., Spira, J., Bazin, H., Szpirer, P., Levan, G. and Klein, G. Rat c-myc oncogene is located on chromosome 7 and rearranges in immunocytomas with t (6:7) chromosomal translocation. Nature 306: 497-498 (1983).

59. Burns, F.J. and Albert, R.E. Radiation carcinogenesis in rat skin. In: Radiation Carcinogenesis (Eds., A.C. Upton, R.E. Albert, F.J. Burns and R.E. Shore), Elsevier, New York, 1986, pp. 199-214.

60. Ormerod, M.G. Radiation-induced strand breaks in the DNA of mammalian cells. In: Biology of Radiation Carcinogenesis (Eds., J.M. Yuhas, R.W. Tennant and J.D. Regan), Raven Press, New York, pp. 67-92, 1976.

61. Burns, F.J. and Sargent, E.V. The induction and repair of DNA breaks in rat epidermis irradiated with electrons. Radiat. Res. 87: 137-144 (1981).

B. Bibliography (publications from closely related projects):

1. Garte, S.J., M.J. Sawey and F.J. Burns. Oncogenes activated in radiation-induced rat skin tumors. In: Radiation Carcinogenesis and DNA Alterations (F.J. Burns, A.C. Upton and G. Silini, Eds.) Plenum Inc., New York, 1986, pp. 389-397.

2. Sawey, M.J., A.T. Hood, F.J. Burns and S.J. Garte. Activation of C-myc and C-K-ras oncogenes in primary rat tumors induced by ionizing radiation. Mol. and Cell. Biol. 7: 932-935 (1987).

3. Sargent, E.V. and F.J. Burns. The early and late effect of ultraviolet light exposure on the induction and repair of electron-induced DNA damage in rat epidermis. Mechanisms of Aging and Development 39: 233-243 (1987).

4. Garte, S.J., M.J. Sawey, F.J. Burns, M. Felber and T. Ashkenazi-Kimmel. Multiple oncogene activation in a radiation carcinogenesis model. In: Anticarcinogenesis and Radiation Protection (P. Cerutti, F. Nygaard and P. Simic, Eds.), Plenum, NY, 1987, pp. 341-344.

5. Burns, F.J. Cancer risk associated with therapeutic irradiation of skin. Arch. Dermatol. 125: 979-981 (1989).

6. Burns, F.J., R.E. Albert and S.J. Garte. Multiple stages in radiation carcinogenesis of rat skin. Environ. Health Persp. 81: 67-72 (1989).

7. Burns, F.J. Mouse skin papillomas as a stage in cancer progression. Prog. Clin. Biol. Res. 298: 81-94 (1989).

8. Burns, F.J., R.E. Albert and S.J. Garte. Radiation induced cancer in rat skin. In: Skin Tumors: Experimental and Clinical Aspects (C.J. Conti, et al., Eds.), Raven Press, NY, 1989, pp. 293-319.

9. Burns, F.J., M.J. Sawey, S. Hosselet and S.J. Garte. Risk assessment and multiple stages in radiation carcinogenesis. In: Low-Dose Radiation: Biological Bases of Risk Assessment (K. Baverstock, Ed.) Taylor and Francis Ltd., 1989, pp. 571-582.

Graduate Students Trained: 1 M.S.
1 year of study towards M.S.

END

DATE FILMED

12/18/90